



UNIVERSITY OF LEEDS

This is a repository copy of *Rack Level Study of Hybrid Liquid/Air Cooled Servers: The Impact of Flow Distribution and Pumping Configuration on Central Processing Units Temperature*.

White Rose Research Online URL for this paper:  
<http://eprints.whiterose.ac.uk/148675/>

Version: Accepted Version

---

**Article:**

Kadhim, MA, Kapur, N [orcid.org/0000-0003-1041-8390](https://orcid.org/0000-0003-1041-8390), Summers, JL [orcid.org/0000-0001-8266-5038](https://orcid.org/0000-0001-8266-5038) et al. (1 more author) (2020) Rack Level Study of Hybrid Liquid/Air Cooled Servers: The Impact of Flow Distribution and Pumping Configuration on Central Processing Units Temperature. *Heat Transfer Engineering*, 41 (19-20). pp. 1683-1698. ISSN 0145-7632

<https://doi.org/10.1080/01457632.2019.1640467>

---

© 2019 Taylor & Francis Group, LLC. This is an author produced version of an article published in *Heat Transfer Engineering*. Uploaded in accordance with the publisher's self-archiving policy.

**Reuse**

Items deposited in White Rose Research Online are protected by copyright, with all rights reserved unless indicated otherwise. They may be downloaded and/or printed for private study, or other acts as permitted by national copyright laws. The publisher or other rights holders may allow further reproduction and re-use of the full text version. This is indicated by the licence information on the White Rose Research Online record for the item.

**Takedown**

If you consider content in White Rose Research Online to be in breach of UK law, please notify us by emailing [eprints@whiterose.ac.uk](mailto:eprints@whiterose.ac.uk) including the URL of the record and the reason for the withdrawal request.



[eprints@whiterose.ac.uk](mailto:eprints@whiterose.ac.uk)  
<https://eprints.whiterose.ac.uk/>

**Rack level study of hybrid liquid/air cooled servers: the impact of flow distribution and pumping configuration on central processing units temperature**

Mustafa A. Kadhim<sup>1,2</sup>, Nikil Kapur<sup>1</sup>, Jonathan L. Summers<sup>1</sup> and Harvey Thompson<sup>1</sup>

Corresponding author: Harvey Thompson, School of Mechanical Engineering

University of Leeds, Leeds, LS2 9JT, UK,

Tel: +44(0)113 343 2136, Email: [H.M.Thompson@leeds.ac.uk](mailto:H.M.Thompson@leeds.ac.uk),

1. Institute of Thermofluids, School of Mechanical Engineering, University of Leeds, UK.

2. School of Mechanical Engineering, University of Babylon, Babylon, Iraq.

**ABSTRACT:**

The flow distribution and central processing unit (CPU) temperatures inside a rack of thirty 1U (single rack unit) Sun Fire V20z servers retrofitted with direct to chip liquid cooling and two coolant pumping configuration scenarios (central and distributed) are investigated using the EPANET open source network flow software. The results revealed that the servers in the top of the rack and close to the cooling distribution unit can receive up to 30% higher flow rate than the servers in the bottom of the rack, depending on the pumping scenario. This results in a variation in the CPU temperatures depending on the position in the rack. Optimisation analysis is carried out and shows that increasing the flow distribution manifold's dimensions can reduce the flow variation through the servers and increase the total coolant flow rate in the rack by roughly 10%. In addition, activating the small pumps in the direct to chip liquid cooling loops inside the servers (distributed pumping) resulted in an increase of 2°C in the CPU temperatures at the high computational workload.

## INTRODUCTION

The continued growth in digital services and digital processing capabilities has led to an increased thermal management challenge for datacentres. The operation of the information technology (IT) equipment, which effectively converts the electrical energy into thermal energy continues to be a challenge for the maintenance of datacentres within acceptable thermal limits. Many cooling techniques have been proposed, however, cooling CPUs using liquids has recently received increasing attention due to their favourable thermal properties compared to air [1]. The generated heat by the IT equipment is transported through multiscale subsystems from the heat generation of the CPU transistors and interconnects which occurs at the chip level and then transferred to the server level and rack level before finally being dissipated to the environment through the heat rejection system [2]. This series of multiscale subsystems for transferring the heat has made the thermal management of datacentres challenging for the designers and engineers. One of these challenges is the collection of the heat from the largest heat generating components, the CPUs of the different servers in a single rack based on direct contact liquid cooling (DCLC) systems. Therefore, sufficient flow rate and even flow distribution in the servers is required in order to maintain the temperatures inside the electronics within their design thermal envelope.

Several studies have explored the potential to improve the energy efficiency and increase the performance of DCLC datacentres. These studies can be categorised into those focussing on the outdoor environment and those on the IT environment. The former have focused on implementing and enhancing chiller-less designs of the heat rejection systems

to the environment [3, 4]. However, studies concerning the IT environment can also be divided into two parts depending on the scale of the study, namely server and rack level.

In the area of heat rejection systems, David et al. [5] studied the effect of the operation conditions of flow rates, heat exchanger arrangements, addition of glycol, and weather conditions on the thermal performance of a chiller-less DCLC design. They found that the addition of antifreeze decreases the cooling capacity while the power consumption of the heat rejection system is strongly linked to the weather conditions. Iyengar et al. [6] proposed a thermodynamic model validated by long run experiments to investigate the feasibility of using chiller-less DCLC design for different weather regions. The results showed that this design provides significant energy saving by reducing the cooling energy consumption to about 3.5% of the total power of the datacentre. Parida et al. [7] highlighted the possibility of using a single loop design instead of a dual loop to transfer the heat from the chip to the heat rejection system directly without using intermediate heat exchanger. They found that the power consumption for the single loop is higher than the one for the dual loop under the same ambient and operation conditions due to the lower thermal capacity of the antifreeze. Parida et al. [8] developed an energy efficient servo algorithm, that offers 25% energy saving, to control the power consumption of the cooling system to a minimum based on the targeted supplied temperature to the rack and the ambient conditions.

At the server level, a single server is used in [9] to investigate the potential of improving the cooling performance. Incorporating microchannel and minichannels in cold plates for on-chip cooling applications have provided a significant improvement in the energy efficiency. Kandlikar and Hayner [10] found that the coolant type, pressure, coolant flow

rate, inlet temperature, and material type are the main factors in the cold plate design. Addagatla et al. [11] studied the effect of inlet water temperature on the thermal performance and power consumption of hybrid liquid/air cooled 2OU (OpenU) server for a wide range of CPU workloads and showed that the cooling power consumption decreases from 7.86 to 4.92W when the server inlet temperature increases from 27.5 to 45°C, respectively. Druzhinin et al. [12, 13] found that increasing the inlet water temperature to the RSC Tornado server from 19 to 65°C decreases the computational performance of the server from 2.72 to 2.44 GFLOPS/W while increasing the server power consumption from 365 to 398W, respectively. Sahini et al. [14] investigated the effect of high inlet coolant temperature on the CPU temperatures and static power losses at the Enterprise-class server and found that increasing the inlet water temperature from 25 to 50°C increases the CPU average temperatures by 21°C and the power consumption of the server by about 4%. Ramakrishnan et al. [15] investigated the effect of the coolant flow rate on the thermal resistance of a CoolIT System's DCLC cold plate. They found that increasing the flow rate gives lower thermal resistance at the expense of higher pressure drop and pumping power while the input heat flux was found to not have any effect on the thermal resistance of the cold plate.

At the rack level, a number of servers forming the rack are tested all together regarding its thermal and operational performance. Compared to the large number of studies at the server level, far fewer have considered the rack level. Zeighami et al. [16] proposed a simplified model to calculate the heat recovery of hybrid liquid/air cooled rack level using the Asetek RackCDU D2C™ design. Ovaska et al. [17, 18] studied the effect of increasing the inlet air temperature from 20 to 30°C on the hybrid cooled (CPUs water cooled and

the remaining components are air cooled) Norwegian Stallo supercomputer servers and found that the power required to perform 1 Gigaflop/s of computing increased from 0.93 to 0.94W, respectively.

Providing sufficient flow rate and distributing the flow equally for all the servers in the rack is necessary to maintain the CPU temperatures within their designed conditions. Ellsworth [19] analysed the flow distribution using MacroFlow software in the IBM 775 rack of supercomputer servers. The rack contained 12 servers, 2 bulk power assemblies, a rear door heat exchanger and four pumps connected in parallel. The results showed differences in the flow rate of the identical branches which theoretically had the same pressure drop although the flow rate in these branches was higher than the design minimum requirement. Alkharabsheh et al. [20] carried out an experimental and theoretical analysis on a rack of CoolIT DCLC cooled servers. Their analysis aimed to calculate the pressure drop of each component in the system. They divided the system into three modules: server modules, central distributed modules, and supply and return manifolds. The results showed that 59% of the total pressure drop in the rack is due to the server modules of which only 31% is constituted by the cold plates and 69% is caused by the flexible corrugated pipes, Stäubli valves and fittings. Sahini et al. [21] provided a comparison study of the pumping configuration using central pumps and small pumps inside a mini rack of 2OU servers for different rack inlet temperature. Their results showed that the CPU temperatures are lower for the case when the central pumps are used.

In this paper, thirty 1U Sun Fire V20z servers in a rack is tested in terms of coolant flow rate, pumping configuration and flow distribution. To the authors' knowledge the present work is the first to:

1. Address the effect of the rack flow rate and pumping configurations (centralised and distributed) on the CPU temperatures for different IT workloads;
2. Investigate the flow distribution in the rack and the resultant variation of the CPU temperatures of different servers in different positions in the rack.

## **EXPERIMENTAL SETUP**

The experimental setup, shown in Figure 1, consists of a full configuration of an IT environment formed from a hybrid liquid/air cooled rack, which is connected to an outdoor heat rejection system that is a chiller-less air handling unit (AHU).

### 1. IT environment:

The IT environment consists of the servers, a cooling distribution module that contains a liquid/liquid heat exchanger (CHx40), discharge and collection manifolds and a passive rear door heat exchanger. The rack also contains a network switch, power shelf and rack power supply units (PSUs).

#### a. Servers module

Thirty 1U Sun Fire V20z servers [22], shown in Figure 2a, are used and each server consists of 2 dual core CPUs (2GHz AMD (Advanced Micro devices) Opteron 64-bit CPUs running Ubuntu Linux) as shown in Figure 2b, a hard disk drive (HDD), and 8 DIMMs of installable memory. The first CPU is called the primary (CPU0) CPU and the second is called secondary (CPU1) CPU. Each CPU has its own of random access memory (RAM), which has four slots of a capacity ranging from 256 to 8GB. The term CPU temperature in this paper will refer to the average temperatures of CPU0 and CPU1.

The servers are liquid-cooled using CoolIT System heads (DCLC heads) while the remaining components such as RAM, PSUs, HDDs and other auxiliary components on the printed circuit board are air cooled using two sets of fans as shown in Figure 2a. Each CoolIT System head, Figure 2c, has a small integrated internal pump, which can be configured to operate using power from the server or alternatively the coolant to the DCLC heads is centrally pumped using the pumps in the CHx40 at the top of the rack.

b. Discharge and collection manifolds

The DCLC heads of the servers are connected, using double-blind quick connectors manufactured by Stäubli, at the rear of the rack to the supply and return plenums that work as manifolds. The cooling loops are joined together through two passages: one for the cold supply side and the other one for the hot return side as shown in Figure 3. These manifolds are connected to the secondary loop of a CHx40 heat exchanger. The manifolds are 1.82m long each with square cross section (25×25mm) and made of stainless steel. The manifolds employ dry-break quick connection technology and can accommodate 42 sets of DCLC heads connected in parallel.

c. CHx40 heat exchanger coolant distribution module

The CHx40 heat exchanger module is designed by CoolIT Systems [23] to exchange the thermal load between two loops: an internal loop which is the coolant that flows through the DCLC heads inside the servers and the external loop which is the coolant that transfers the heat away to the outside environment through the AHU (see Figure 1). The CHx40 consists mainly of a plate to plate heat exchanger, two pumps, valves, fittings, a

reservoir, temperature sensors, pressure sensors on both loops, a flow sensor on the secondary loop, and a humidity sensor, as shown in Figure 4.

## 2. Outdoor environment

The external loop of the CHx40 is connected to the AHU to reject the heat to the outside environment. The heat rejection system is a chiller-less bespoke design of AHU that utilises a Carel spray system for evaporative cooling which is located outside of the IT room as shown in Figure 1.

## **METHODOLOGY**

The primary goal of the experiments is to measure CPU temperatures of the servers for different IT workloads under a range of internal, secondary loop flow rates for different pumping configurations. The tested coolant flow rate varies from 4.5 l/min to 13.5 l/min for central pumping and from 7.2 l/min to 15.6 l/min for distributed pumping.

The study is concerned with the components connected in the internal loop of the CHx40. Therefore, temperature, pressure and flow rate sensors are used in the internal loop of the CHx40. Each server has temperature sensors at various locations to measure the component temperatures such as the CPU temperatures. All the sensors are dynamically logged by the master server (eng01) with a network timestamp that can be downloaded and processed later.

The inlet temperature to the CHx40 is chosen to be 20°C to ensure that the inlet temperature to the rack falls within the ASHRAE liquid cooled server envelope (W4) (ranges from 2 to 45°C) [24]. The primary loop flow rate is kept constant at 18l/min for all

the experiments. Three synthetic computational load levels are tested which are idle (0%), 50% and full (100%). Five pump speeds are chosen that give a specific flow rate in each case. Both pumps are set to the same speed in each experiment to keep the redundancy of the pump designs. In the central pumping, the two pumps inside the CHx40 are used to pump the coolant inside the rack and through the CPU cooling units, while in the distributed pumping, the pumps inside the servers at the CPUs heads are running in addition to the central pumps.

The experimental process for each case is started by setting the inlet temperature to the CHx40, then loading the rack with a specified synthetic computation load. At this point, the chosen secondary loop flow rate is set. The test for each flow rate runs for 60 minutes before changing the pump speed for the next test. The data is collected and averaged for the last 15 minutes as the steady state is reached by that time.

## **FLOW ANALYSIS**

Uniform flow distribution of the coolant in the servers of the rack increases the reliability of the server operation by providing sufficient coolant flow rate. The flow distribution inside the rack is analysed using the open source EPANET 2.0 software [25] which allows simulation of water hydraulic behaviour and quality within pipe networks. The EPANET software is based on analytical experiments for major and minor losses on the pipe networks.

The network representation of the secondary loop system is simulated for the two types of pumping configurations. The properties of each component in the loop are defined in terms of minor loss coefficient, friction factor, length of the pipe, diameter, elevation of

every node, and pump characteristic curves. The secondary loop conditions are divided into three sections:

### 1. DCLC heads

The number of the DCLC heads is 30 pairs which represents the whole rack. Each DCLC head is represented as a pipe of equivalent head losses in the case of central pumping and represented as a two pipe segment connected by two pumps in series in the distributed pumping case, as shown in Figure 5. The DCLC head pump curve is fed into the software in the case of distributed pumping. The minor losses coefficient in the DCLC heads are taken from a recent study by Alkharabsheh et al. [20] where they analysed the pressure drop in a direct liquid cooled rack. The DCLC heads are assumed identical in the present analysis. Table 1 shows the conditions that define the server modules in the EPANET software.

### 2. Discharge and collection manifolds

Each manifold is divided into 42 section to represent the Stäubli valves T-junctions. The manifolds have square cross section, thus the characteristic hydraulic diameter is used in the software. The pressure losses in the manifolds are calculated based on the two losses coefficients, a major one due to the friction, and a minor one due to the change in the flow direction and T-junction losses. The minor losses coefficient is fed into the EPANET software using standard tables [26]. Table 2 shows the conditions that define the manifolds.

### 3. CHx40 module unit

The secondary loop of the CHx40 contains mainly pipes, fittings, Stäubli valves, a tank, two pumps and a heat exchanger loop. The tank and the two pumps are physically represented in the modelling while the other components are represented by the head losses. The pump characteristic curves are fed into the program, and every pump has five curves depending on the speed settings used, as shown in Figure 6. The tank in the CHx40 is of rectangular shape with dimensions of  $(30 \times 15 \times 10 \text{ cm}^3)$ , hence the tank is fed as a cylindrical reservoir to the software with an equivalent diameter ( $D_{eq}$ ) of 19.53cm, calculated using the equation  $D_{eq} = 1.128 \times \sqrt{W \times L}$ , where W and L are the width and length of the tank . Table 3 shows the conditions that define the reservoir characteristics.

## **MODEL VALIDATION**

The model is validated against the experimental results for the centralised and distributed pumping cases for the five CHx40 pump speeds and also for the case where the CHx40 pumps are deactivated. Figures 7 and 8 show that the EPANET software models the flow inside the rack with good accuracy, with an average discrepancy of 2.3% compared with the experimental results for the two pumping cases. These figures represent the relationship between the total coolant flow rate and the pump speed. The central pumps inside CHx40 have five different speeds with pump speed 0 representing the point where both of the pumps are off.

## **FLOW DISTRIBUTION IN THE RACK**

The calculated flow distribution in the rack is presented for the centralised pumping configuration in Figure 9. It can be seen that the flow through servers at the top of the rack are larger than those located at the bottom of the rack. The calculations are based

on the assumption that all the DCLC heads have the same pressure drop resistance which is due to the major and minor losses caused by the Stäubli valves, the flexible corrugated hoses, and the microchannels of the cold plates. As a result, the flow rate variation through different servers is only caused by the frictional losses in the supply and collection manifolds of the rack. These losses are caused by the friction between the coolant and the internal manifold surface and the change of the flow direction from the manifolds to the DCLC heads of the servers.

The results of the simulations show that the server at the top of the rack (eng01) receives the coolant with a 28% higher flow rate than the server in the bottom of the rack (eng30) when the CHx40 pumps are at the highest speed (pump speed 5). This variation reduces to about 24% at the lowest pump speed (pimp speed 1). The results also show that the differences between pump speed 4 and 5 are minimal. Since the total flow affects the heat transfer characteristics, with larger flows having a lower thermal resistance and a greater thermal capacity then this corresponds with servers at the top of the rack having a lower CPU temperature than those towards the bottom of the rack.

The flow distribution in the distributed pumping configuration is shown in Figure 10. The flow maldistribution in the distributed pumping configuration is higher than for the centralised pumping case. The flow rate received by the server at the top of the rack (eng01) is 33% higher than for the lowest server (eng30) in the rack. The differences decrease when reducing the CHx40 pump speeds with a minimum of 24% when the CHx40 pumps are turned off.

The flow rates through the bottom ten servers in the rack are the same for both cases of centralised and distributed pumping configurations. It follows that, the CPUs of the lower ten servers in the bottom of the rack should have the same temperature as the flow rate across these 10 servers has little variation.

## **CPU TEMPERATURE VARIATIONS**

The average CPU temperature distribution of all the servers at 100% utilisation workload is shown in Figure 11 with the highest central pump speed (pump speed 5). The general trend of the CPU temperatures shows that the servers at the top of the rack have lower temperature than the servers in the bottom of the rack. Statistical analysis of the data shows that the temperature distribution can be represented by a quadratic model with a regression factor of 0.72.

The temperature distribution of the CPUs of different servers in the rack at idle operation is shown in Figure 12. The CPU temperatures shows high variation between the different servers in the rack and the effect of flow distribution is insignificant and outweighed by other factors such as the pressure drop variation in the DCLC heads of different servers.

The results of temperature variations under the same load particularly in the last ten servers of the rack, which theoretically have the same flow rate, indicate that there are other factors which are also affecting the flow distribution and in turn the different CPU temperatures. Therefore, the experimental CPU temperatures are shown against the calculated theoretical server flow rates to estimate the effect of the flow distribution on the CPU temperature variations.

The CPU temperatures as a function of server flow rate is shown in Figure 13 for 100% computational workload. The servers of lower flow rate, which are the servers in the bottom of the rack, have temperature variations from about 47 to 54°C even if the flow rate is the same. This issue is attributed to different factors such as the placement of the DCLC head over the CPU, different thermal interface materials which causes different thermal resistances between the chip and the coolant for different servers, and the corrosion and blockage that may occur in the microchannel of the cold plate of the DCLC head. This is supported by a recent study by Alkharabsheh et al. [20] where they found that the DCLC heads have different flow resistance and that the position of the corrugated tubes also has a large effect on the pressure drop of the DCLC head. The temperature variation can also be attributed to the fact that the thermal behaviour of the CPUs is not always consistent.

The relationship between the CPU temperatures and the flow rate through the DCLC heads can be best fitted with a polynomial fitting curve of second order with a regression factor of 0.47. The low regression factor is also attributed to the aforementioned factors that results in different CPUs temperature for the same flow rate through the DCLC heads of different servers.

The CPU temperatures as a function of the calculated flow rate for the idle operation of the servers is shown in Figure 14. The decrease in the CPU temperatures as a function of increasing the server flow rate is within the CPU temperature variation for the same flow rate. Therefore, it is difficult to evaluate the effect of flow variation on the CPUs temperature in the idle case as the CPUs of the servers have relatively lower temperature.

However, the general trend of the CPU temperatures is still decreasing with the increasing server flow rates.

## **OPTIMISATION OF THE DESIGN**

Optimising the DCLC rack design should take two paths: improving the DCLC head design to reduce the pressure drop in these segments of the loop and improving the design of the discharge and collection manifolds. The scope of the current study will focus on optimising the manifolds design. This is obtained by examining the effect of the equivalent diameter of the discharge and collection sections of the manifolds on the flow distribution and total rack flow rate.

The resultant improvement between the flow distribution and the equivalent manifold diameter as well as the improvement in the total loop flow rate for the centralised and distributed pumping are shown in Figures 15 and 16, respectively. The results of the optimisation shows that increasing the manifolds equivalent diameter from 2.5 to 5cm reduces the difference between the flow rates of servers eng01 and eng30 from 28% to 2% and from 33% to 2% for the centralised and distributed pumping, respectively. The total rack flow rate improves by 9% and 10% for the centralised and distributed pumping, respectively.

## **CENTRALISED AND DISTRIBUTED PUMPING**

This section presents experimental results of the effect of the pumping configuration and the flow rate on the CPU temperatures. Four servers are selected: eng02, eng10, eng20 and eng30.

As shown in Figure 17 to 19, the CPU temperatures are on average higher for the distributed pumping (DP) than the centralised pumping (CP) for the same flow rate. The differences between the CPU temperatures in the DP and the CP configurations are within the percentage error for the four selected servers in the idle case as shown in Figure 17. However, these differences are shown to be 1.5°C on average when the servers are stressed with 50% workload (Figure 18), increasing to 2°C under full workload (Figure 19).

The improvement in the CPU temperatures with increasing coolant flow rate is relatively small for the idle case and within 1°C for both the CP and DP configurations, as shown in Figure 17. However, for the 50% synthetic workload of the rack shown in Figure 18, the CPU temperatures were found to decrease by 4.2% on average when the flow rate is increased from 4.7 l/min to 13.5 l/min for the CP case and by 5.5% when the flow rate is increased from 7.2 to 15.8 l/min for the DP case. Moreover, at the full workload of the servers shown in Figure 19, the average reduction in the CPU temperatures is 6% when increasing the pump speed from 4.3 to 13.7 l/min for the CP configuration and 5% when increasing the flow rate from the 7.5 to 15.8 l/min for the DP configuration.

It should be mentioned that two of the servers encountered overheating and shutdown during the high load level of operation with the low flow rate in the CP configuration. However, for the DP configuration, all the servers remained within the safe range of CPU temperatures even at the lower flow rate where the CHx40 pumps were deactivated. Therefore, activating the DCLC head pumps could be automated with an algorithm to activate the pump when the CPU of a particular server reaches the warning temperature so that the pressure drop is reduced and the flow rate through the server is increased.

## CONCLUSIONS

This paper aimed to provide new understanding of the issue of flow maldistribution in distributed direct to chip liquid cooling and its relationship with CPU temperature variations. The design was optimised to obtain uniform flow through all the servers in the rack. Moreover, the coolant pumping configuration and the effect of flow rate in the rack on CPU temperatures was also investigated for various IT loads.

The EPANET open source software was used to analyse the flow in the rack for two types of pumping configurations: centralised and distributed pumping. The model predicted the flow rate in the rack with an accuracy of 2.3% compared with the experimental results. The results of the analysis showed that the server in the top of the rack (eng01) receives a 28% higher flow rate and 33% more than the server in the bottom of the rack (eng30) for the centralised and distributed pumping, respectively. The differences in the coolant flow rate received by every server resulted in a general increase in the CPU temperatures of the servers between the top and the bottom of the rack.

The friction losses of the manifolds leads to variation of the flow rate of different servers in the rack. Therefore, optimisation analysis showed that increasing the manifolds' hydraulic diameter from 2.5 to 5cm provides more uniform flow for all the servers and enhances total rack flow rate by around 10%.

The CPU temperatures in the rack were found to be higher by 2°C for the distributed pumping compared with the centralised pumping for the same flow rate at the high IT workloads. Increasing the total flow rate of the rack showed less effect on the component

temperatures at the low level workloads while it was more significant for the high level workloads.

## **DISCLAIMER**

The CoolIT System components used in this work are from an earlier system design and do not necessarily imply that current versions behave in the same manner.

## **ACKNOWLEDGMENTS**

The authors would like to thank Airedale International Air Conditioning Ltd., for the collaboration and providing the dry air-cooler modified with a Carel spray system. We would like to acknowledge the Advanced Research Computing unit from the University of Leeds for donating the Sunfire V20z systems. We would like to thank CoolIT systems for providing the liquid cooling systems used. MK would like to thank the Iraqi Ministry of Higher Education for funding his PhD research.

## **NOMONCLATURE**

AHU	Air handling unit
ASHRAE	American society of heat refrigeration and air conditioning engineering
CHx40	Liquid-liquid heat exchanger
CP	Central pumping
CPU	Central processing unit
DCLC	Direct contact liquid cooling

$D_{eq}$	Equivalent diameter
DP	Distributed pumping
eng	Server (eng01 means server 01, eng02 means server 02 and so on)
IT	Information technology
L	Length of the tank
PSU	Power supply unit
Qs	Secondary flow rate
RAM	Random-access memory
U	Single rack unit (44.45mm)
W	Width of the tank

## REFERENCES

- [1] R. C. Chu, R. E. Simons, M. J. Ellsworth, R. R. Schmidt, and V. Cozzolino, "Review of cooling technologies for computer products," *IEEE Transactions on Device and materials Reliability*, vol. 4, no. 4, pp. 568-585, 2004. DOI:10.1109/TDMR.2004.840855.
- [2] J. D. Rambo, "Reduced-order modeling of multiscale turbulent convection: application to data center thermal management," Ph.D. dissertation, School of Mechanical Engineering, Georgia Institute of Technology, Georgia, USA, 2006.
- [3] M. A. Kadhim, Y. T. Al-Anii, N. Kapur, J. L. Summers, and H. M. Thompson, "Performance of a mixed mode air handling unit for direct liquid-cooled servers." presented at the 33rd Thermal Measurement, Modeling & Management Symposium (SEMI-THERM), San Jose, CA, USA, March 13-17, 2017.
- [4] R. C. Chu, M. K. Iyengar, V. Kamath, and R. R. Schmidt, "Energy efficient apparatus and method for cooling an electronics rack," Google Patents, 2010.
- [5] M. P. David, M. K. Iyengar, P. Parida, R. E. Simons, M. Schultz, M. Gaynes, R. Schmidt, and T. Chainer, "Impact of operating conditions on a chiller-less data center test facility with liquid cooled servers." presented at the 13th InterSociety Conference on Thermal and Thermomechanical Phenomena in Electronic Systems, San Diego, CA, USA, 30 May-1 June 2012.
- [6] M. Iyengar, et al., "Extreme energy efficiency using water cooled servers inside a chiller-less data center." presented at the 13th InterSociety Conference on Thermal and Thermomechanical Phenomena in Electronic Systems, San Diego, CA, USA, 30 May-1 June 2012.

- [7] P. R. Parida et al., "System-Level Design for Liquid Cooled Chiller-Less Data Center." presented at ASME 2012 International Mechanical Engineering Congress and Exposition, Texas, USA, November 9–15, 2012.
- [8] P. R. Parida, T. J. Chainer, M. D. Schultz, and M. P. David, "Cooling Energy Reduction during dynamically controlled data center operation." presented at ASME 2013 International Technical Conference and Exhibition on Packaging and Integration of Electronic and Photonic Microsystems, Burlingame, California, USA, July 16–18, 2013.
- [9] G. I. Meijer, "Cooling energy-hungry data centers," *Science*, vol. 328, no. 5976, pp. 318-319, 2010. DOI: 10.1126/science.1182769.
- [10] S. G. Kandlikar, and C. N. Hayner, "Liquid cooled cold plates for industrial high-power electronic devices—Thermal design and manufacturing considerations," *Heat Transfer Engineering*, vol. 30, no. 12, pp. 918-930, 2009. DOI: 10.1080/01457630902837343.
- [11] A. Addagatla, J. Fernandes, D. Mani, D. Agonafer, and V. Mulay, "Effect of warm water cooling for an isolated hybrid liquid cooled server." presented at the 2015 31st Thermal Measurement, Modeling & Management Symposium (SEMI-THERM), San Jose, CA, USA, 15-19 March 2015.
- [12] E. Druzhinin et al., "High temperature coolant demonstrated for a computational cluster." presented at the 2016 International Conference on High Performance Computing & Simulation (HPCS), Innsbruck, Austria, 18-22 July 2016.
- [13] E. A. Druzhinin, A. B. Shmelev, A. A. Moskovsky, V. V. Mironov, and A. Semin, "Server Level Liquid Cooling: Do Higher System Temperatures Improve Energy

- Efficiency?," Supercomputing frontiers and innovations, vol. 3, no. 1, pp. 67-74, 2016. DOI: 10.14529/jsfi160104.
- [14] M. Sahini et al., "Comparative study of high ambient inlet temperature effects on the performance of air vs. liquid cooled IT equipment." presented at the 2017 16th IEEE Intersociety Conference on Thermal and Thermomechanical Phenomena in Electronic Systems (ITherm), Orlando, FL, USA, 30 May-2 June 2017.
- [15] B. Ramakrishnan et al., "Experimental characterization of a cold plate used in warm water cooling of data centers." 2017 33rd Thermal Measurement, Modeling & Management Symposium (SEMI-THERM), San Jose, CA, USA, 13-17 March 2017.
- [16] R. Zeighami, W. A. Saunders, H. Coles, and S. Branton, "Thermal performance modeling of hybrid liquid-air cooled servers." presented at the Fourteenth Intersociety Conference on Thermal and Thermomechanical Phenomena in Electronic Systems (ITherm), Orlando, FL, USA, 27-30 May 2014.
- [17] S. J. Ovaska, R. E. Dragseth, and S. A. Hanssen, "Impact of retrofitted CPU water cooling on supercomputer performance and power consumption." SoutheastCon 2016, Norfolk, VA, USA, 30 March-3 April 2016.
- [18] S. J. Ovaska, R. E. Dragseth, and S. A. Hanssen, "Direct-to-chip liquid cooling for reducing power consumption in a subarctic supercomputer centre," International Journal of High Performance Computing and Networking, vol. 9, no. 3, pp. 242-249, 2016.
- [19] M. J. Ellsworth, "Flow network analysis of the IBM power 775 supercomputer water cooling system." presented at the fourteenth Intersociety Conference on Thermal

- and Thermomechanical Phenomena in Electronic Systems (ITherm), Orlando, FL, USA, 27-30 May 2014.
- [20] S. Alkharabsheh, B. Ramakrishnan, and B. Sammakia, "Pressure drop analysis of direct liquid cooled (DLC) rack." presented at the 16th IEEE Intersociety Conference on Thermal and Thermomechanical Phenomena in Electronic Systems (ITherm), Orlando, FL, USA, 30 May-2 June, 2017. pp. 815-823.
- [21] M. Sahini et al., "Rack-level study of hybrid cooled servers using warm water cooling for distributed vs. centralized pumping systems." presented at 33rd Thermal Measurement, Modeling & Management Symposium (SEMI-THERM), San Jose, CA, USA, 13-17 March 2017.
- [22] Sun Microsystems, Sun Fire V20z and Sun Fire V40z Servers. Server Management Guide. Sun Microsystems, Inc., 4150 Network Circle, Santa Clara, California 95054, U.S.A, 2005.
- [23] CoolIT. available from: <http://www.coolitsystems.com/>.
- [24] ASHRAE Technical Committee, Thermal guidelines for data processing environments-expanded data center classes and usage guidance. American Society of Heating, Refrigerating and Air-Conditioning Engineers, ASHRAE datacom series book 1, Atlanta, 2011.
- [25] L. A. Rossman, EPANET 2: users manual. national risk management research laboratory office of research and development u.s. environmental protection agency cincinnati, ohio, USA, 2000.
- [26] Y. A. Cengel, and J. M. Cimbala, "Fluid Mechanics. Vol. 1," Tata McGraw-Hill Education, New York, 2006.

[27] Xylem Inc. "D5 series," available from <https://www.hvacquick.com/>. Accessed: April. 22, 2019.

**Table 1: DCLC head properties in EPANET**

Number of server modules	Diameter (mm)	Pipe length (m)	Losses coefficient	Roughness coefficient
30	6	2.45	350	0.001524

**Table 2: Properties of the two manifolds in EPANET**

Number of segments	Hydraulic diameter (mm)	Segment length (mm)	Losses coefficient	Roughness coefficient
84	25	45	4	0.072

**Table 3: Properties of the reservoir in EPANET**

Equivalent diameter (cm)	Max level (mm)	Min level (mm)	Initial level (mm)	Elevation (m)
19.53	100	0	80	2.1

## LIST OF FIGURE CAPTIONS

Figure 1 Diagram of the full design configuration of DCLC chiller less cooled rack.

31

Figure 2 (a) Sun Fire V20z server with DCLC units, (b) CPU before placing the DCLC head and (c) the DCLC head assembly. 32

Figure 3 Back of the rack showing the manifolds and DCLC Stäubli valves connections.

33

Figure 4 CHx40 liquid to liquid heat exchanger, available in the public domain from coolIT ([https://www.coolitsystems.com/company/chx40\\_screenon/](https://www.coolitsystems.com/company/chx40_screenon/)) [23]. 34

Figure 5 Secondary loop design in EPANET software: (a) centralised and (b) distributed pumping. 35

Figure 6 Laing Thermotech pump characteristic curve used in the CHx40, available in the public domain ([https://www.hvacquick.com/catalog\\_files/Laing\\_D5\\_Vario\\_Catalog.pdf](https://www.hvacquick.com/catalog_files/Laing_D5_Vario_Catalog.pdf)) [27]. 36

Figure 7 Validation of the calculated loop flow rate using the EPANET software against the experimental data for the central pumping case. 37

Figure 8 Validation of the calculated loop flow rate using the EPANET software against the experimental data for the distributed pumping case. 38

Figure 9 Rack flow distribution in the centralised pumping case. 39

Figure 10 Rack flow distribution in the distributed pumping case. 40

Figure 11 CPUs Temperature distribution of the servers at 100% load operation, the fitting curve represents the trend of variation of the CPUs temperature from the top to the bottom of the rack. 41

Figure 12 CPUs Temperature distribution of the servers in idle operation. 42

Figure 13 Average CPUs temperature as a function of the server flow rate at 100% stress level of the rack. 43

Figure 14 Average CPUs temperature as a function of the server flow rate at idle operation of the rack. 44

Figure 15 Manifold size effect on the flow distribution in the central pumping configuration (the CHx pumps are running only). 45

Figure 16 Manifold size effect on the flow distribution in the distributed pumping configuration (the CHx pumps are kept running as well as the small pumps at the CPUs). 46

Figure 1 Average temperature of selected CPUs as a function of the secondary loop flow rate for the idle operation of the rack. (The numbers in the legend are referred to the servers number from the top to the bottom of the rack while the CP and DP are referred to the centralised and distributed pumping configurations). 47

Figure 28 Average temperature of selected CPUs as a function of the secondary loop flow rate for the 50% workload. (The numbers in the legend are referred to the servers number from the top to the bottom of the rack while the CP and DP are referred to the centralised and distributed pumping configurations). 48

Figure 19 Average temperature of selected CPUs as a function of the secondary loop flow rate for the 100% workload. (The numbers in the legend are referred to the servers number from the top to the bottom of the rack while the CP and DP are referred to the centralised and distributed pumping configurations). 49

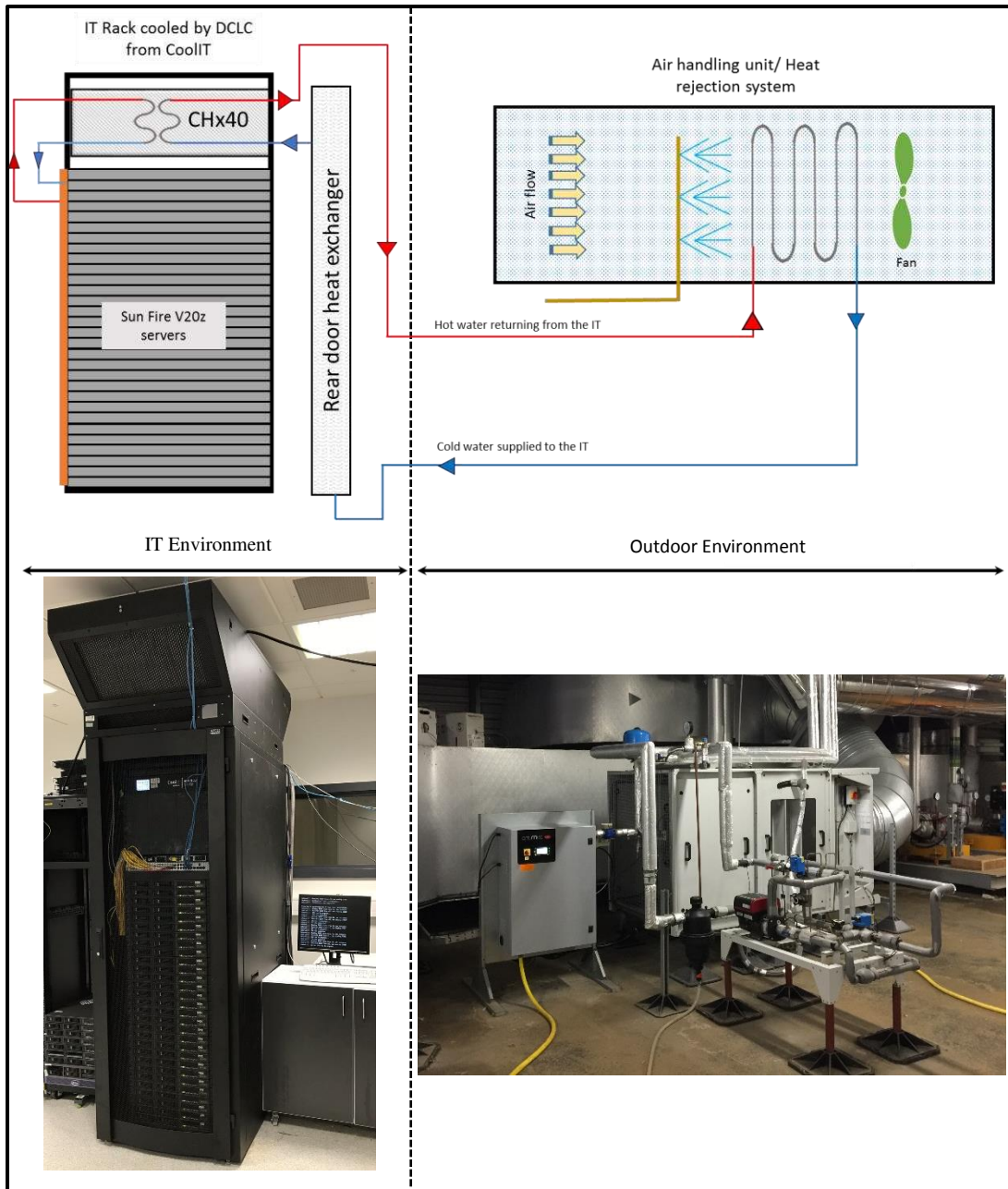


Figure 3 Diagram of the full design configuration of DCLC chiller less cooled rack

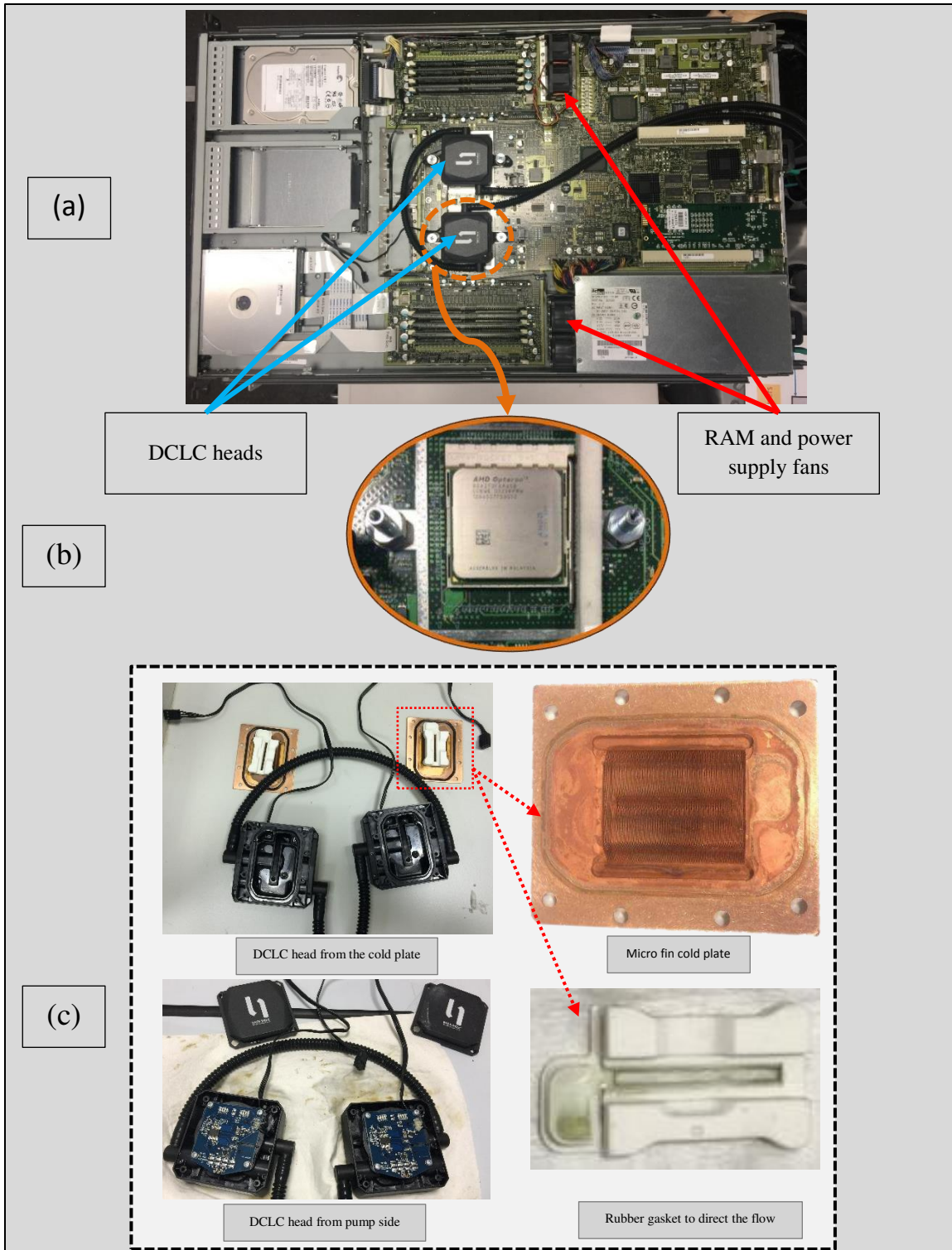
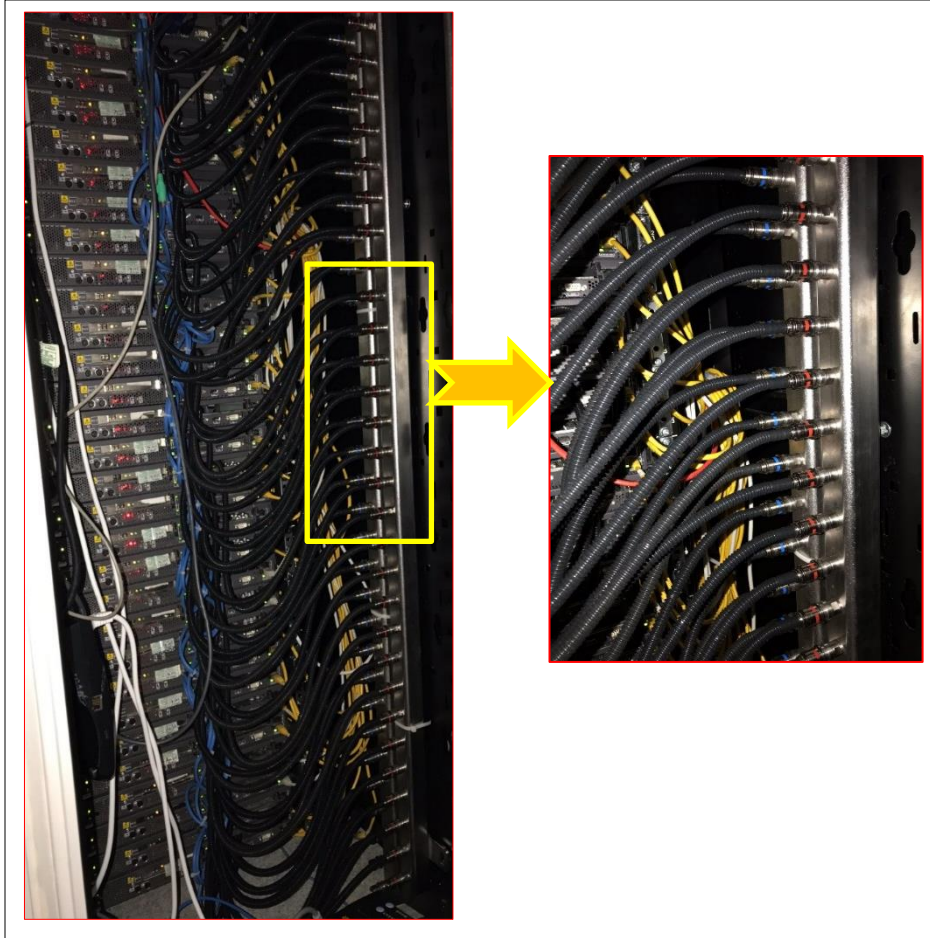


Figure 4 (a) Sun Fire V20z server with DCLC units, (b) CPU before placing the DCLC head and (c) the DCLC head assembly.



**Figure 5 Back of the rack showing the manifolds and DCLC Stäubli valves connections.**

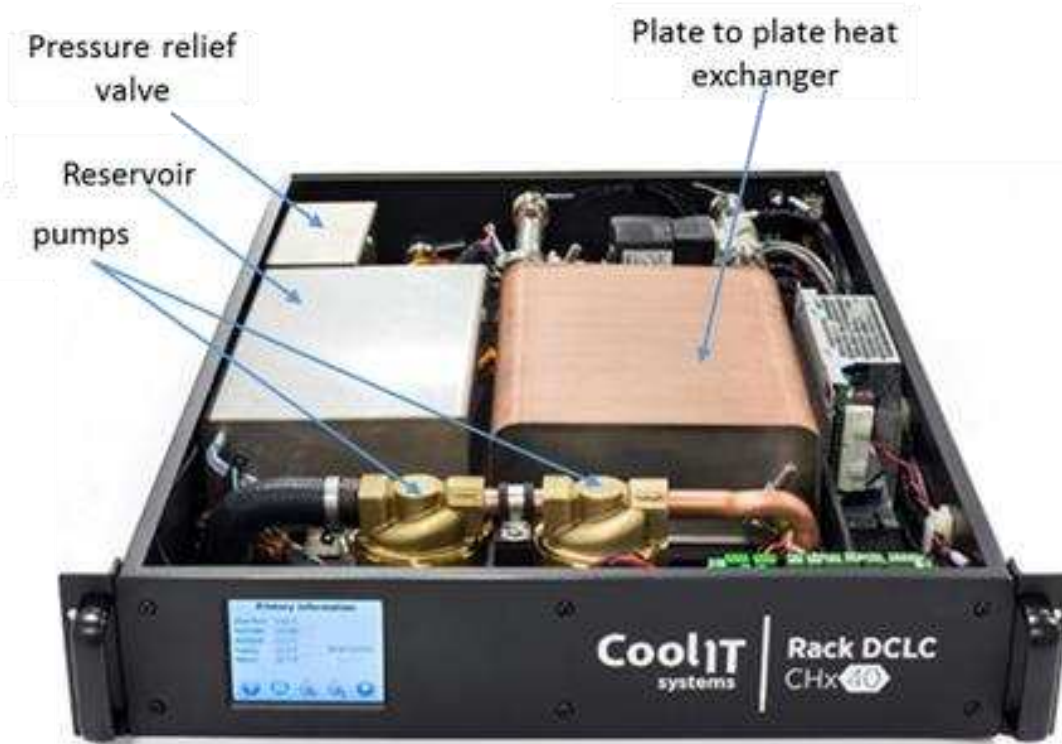
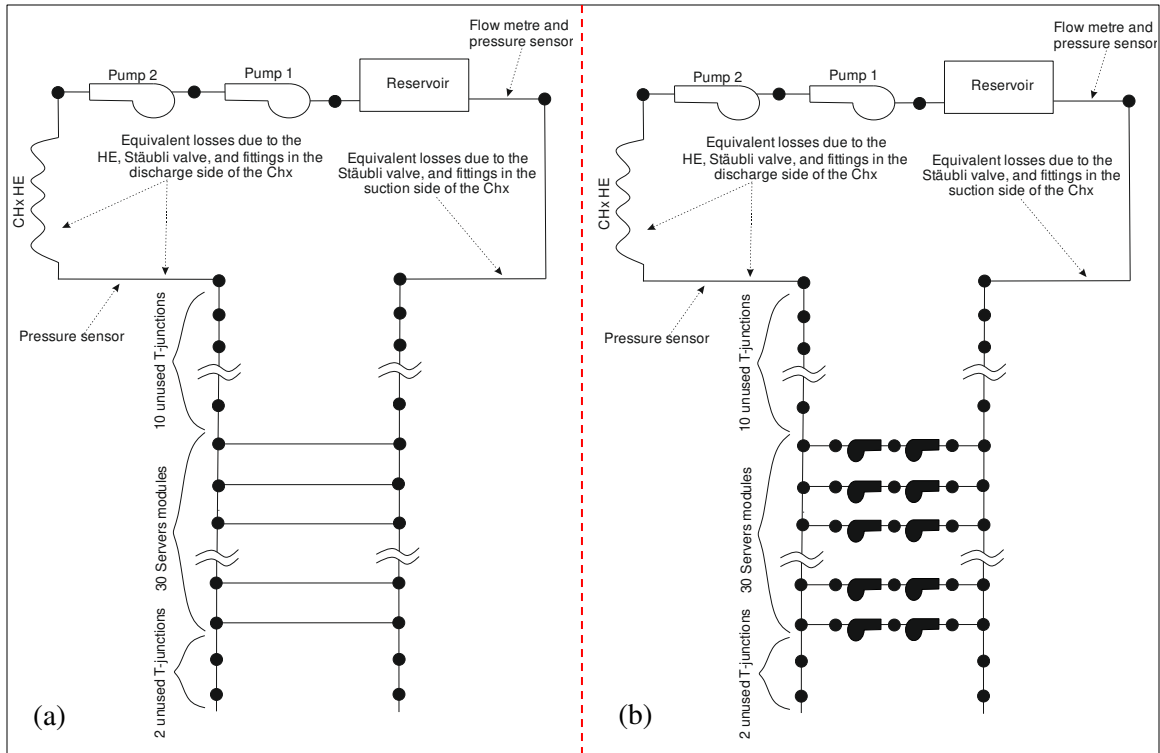
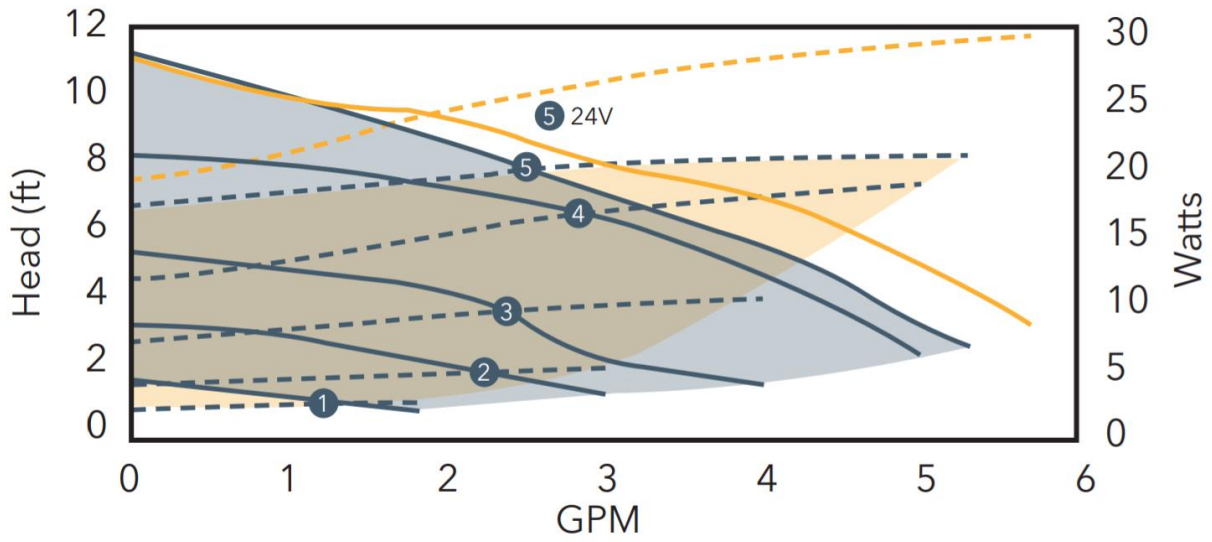


Figure 6 CHx40 liquid to liquid heat exchanger, available in the public domain from coolIT ([https://www.coolitsystems.com/company/chx40\\_screenon/](https://www.coolitsystems.com/company/chx40_screenon/))

[23].



**Figure 7 Secondary loop design in EPANET software: (a) centralised and (b) distributed pumping.**



**Figure 8 Laing Thermotech pump characteristic curve used in the CHx40,  
available in the public domain**

[https://www.hvacquick.com/catalog\\_files/Laing\\_D5\\_Vario\\_Catalog.pdf](https://www.hvacquick.com/catalog_files/Laing_D5_Vario_Catalog.pdf) [27].

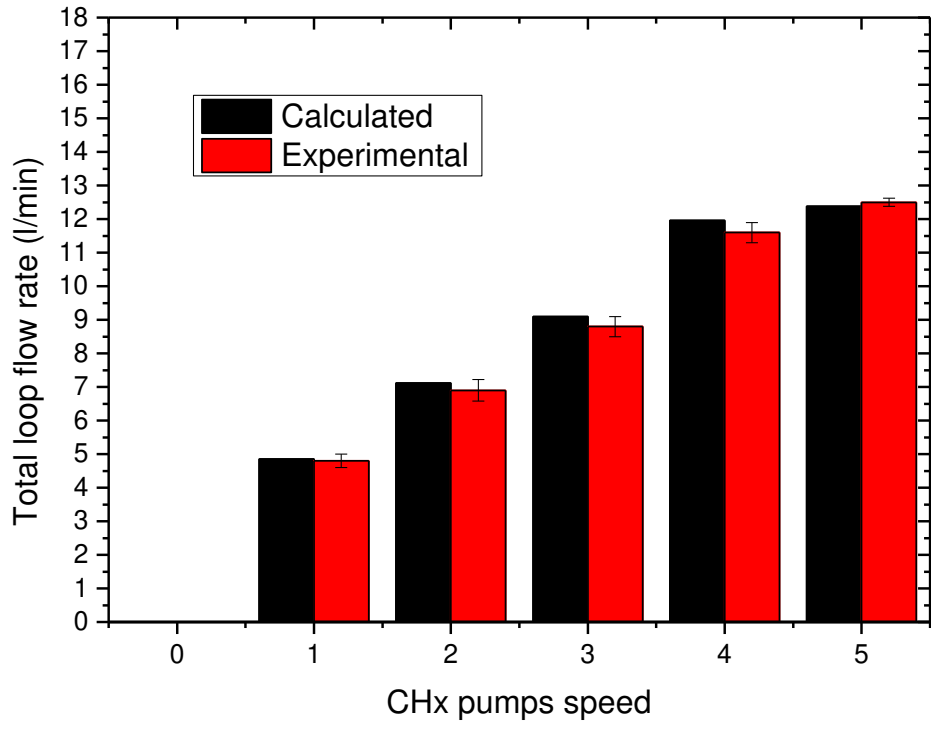


**Figure 9 Validation of the calculated loop flow rate using the EPANET software against the experimental data for the central pumping case.**

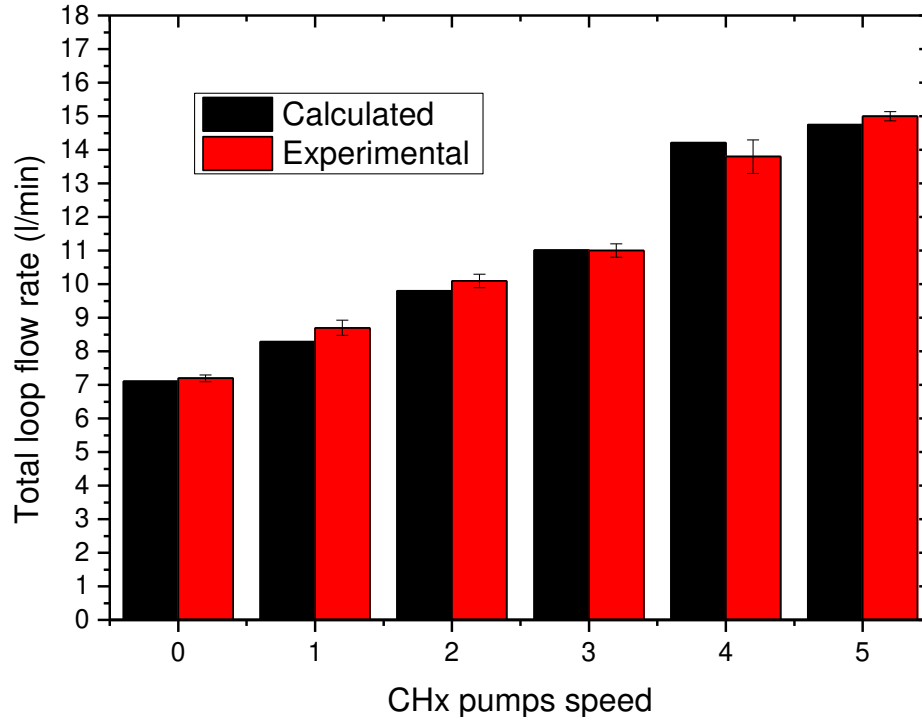


**Figure 10 Validation of the calculated loop flow rate using the EPANET software against the experimental data for the distributed pumping case.**

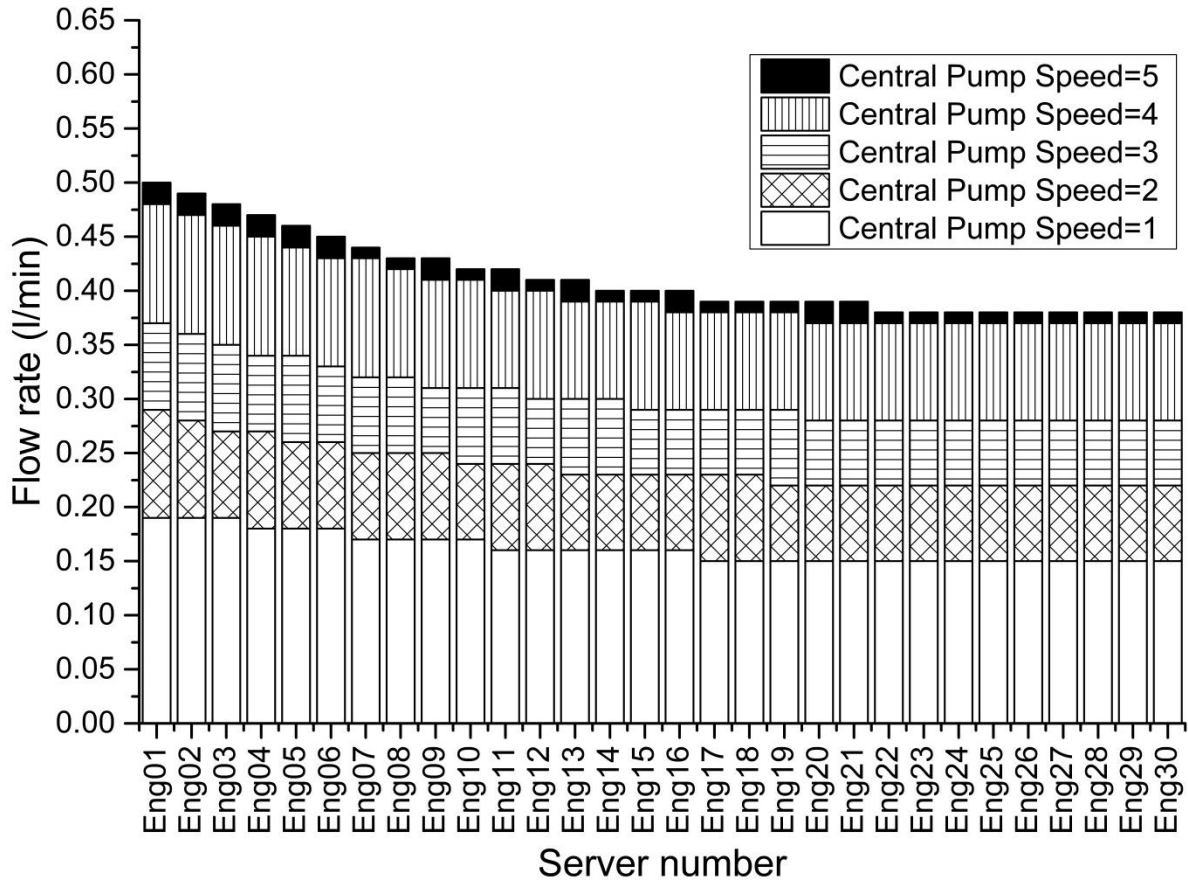


**Figure 11 Rack flow distribution in the centralised pumping case.**

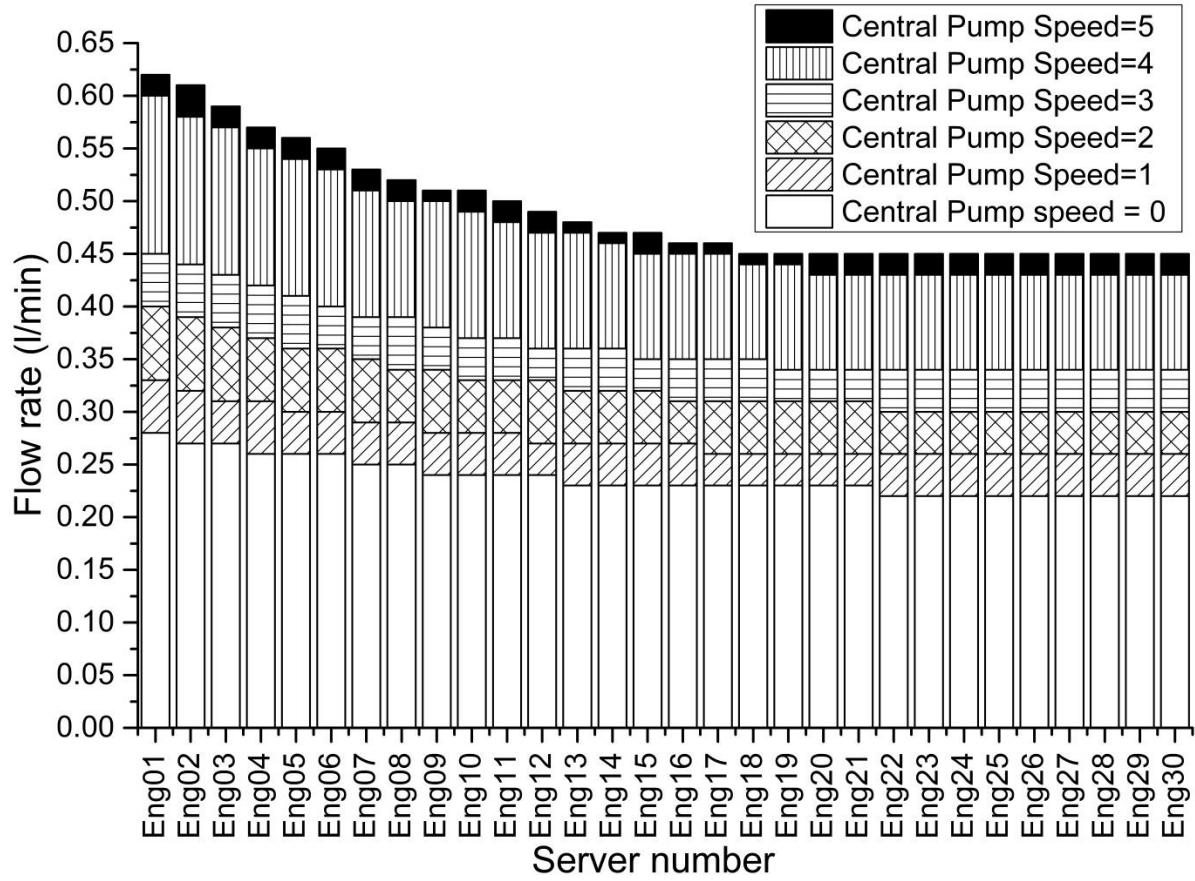
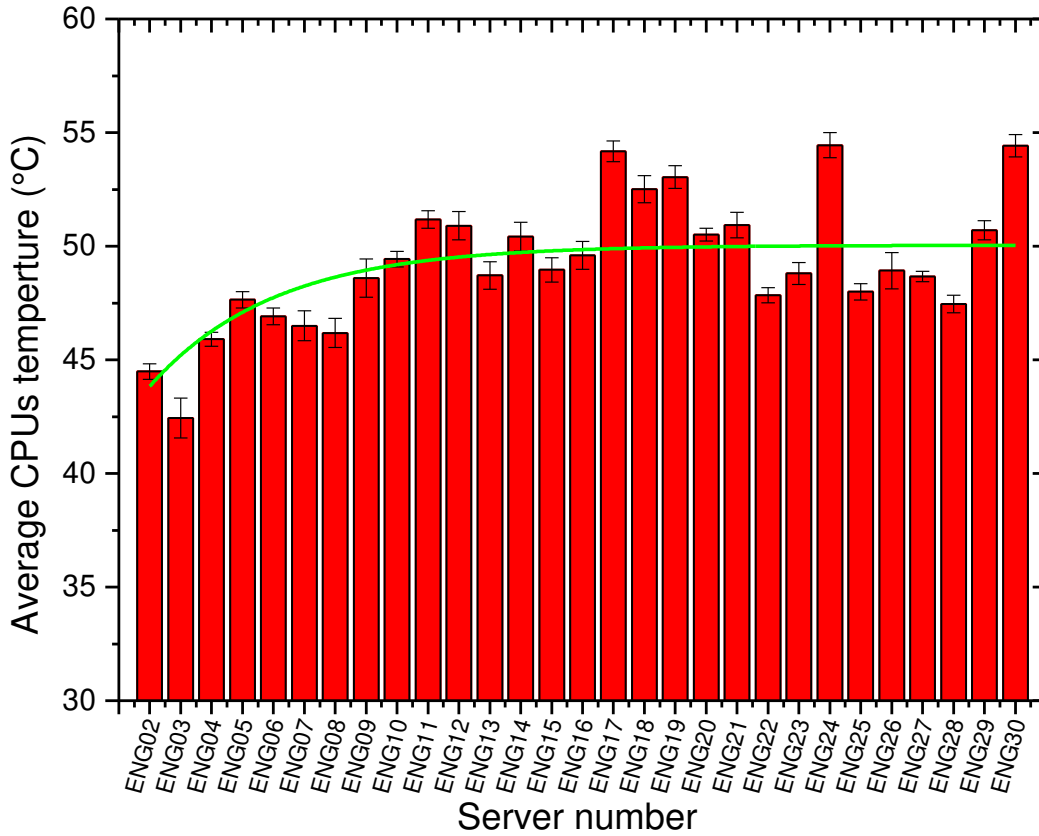
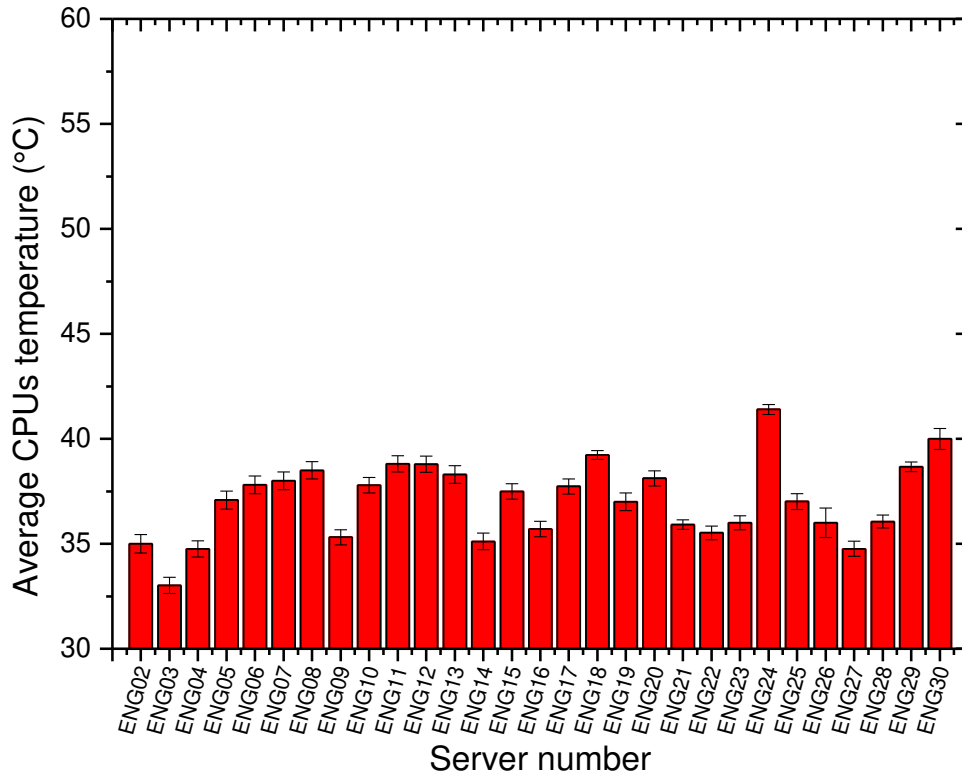


Figure 12 Rack flow distribution in the distributed pumping case.



**Figure 13 CPUs Temperature distribution of the servers at 100% load operation, the fitting curve represents the trend of variation of the CPUs temperature from the top to the bottom of the rack.**



**Figure 14 CPUs Temperature distribution of the servers in idle operation.**

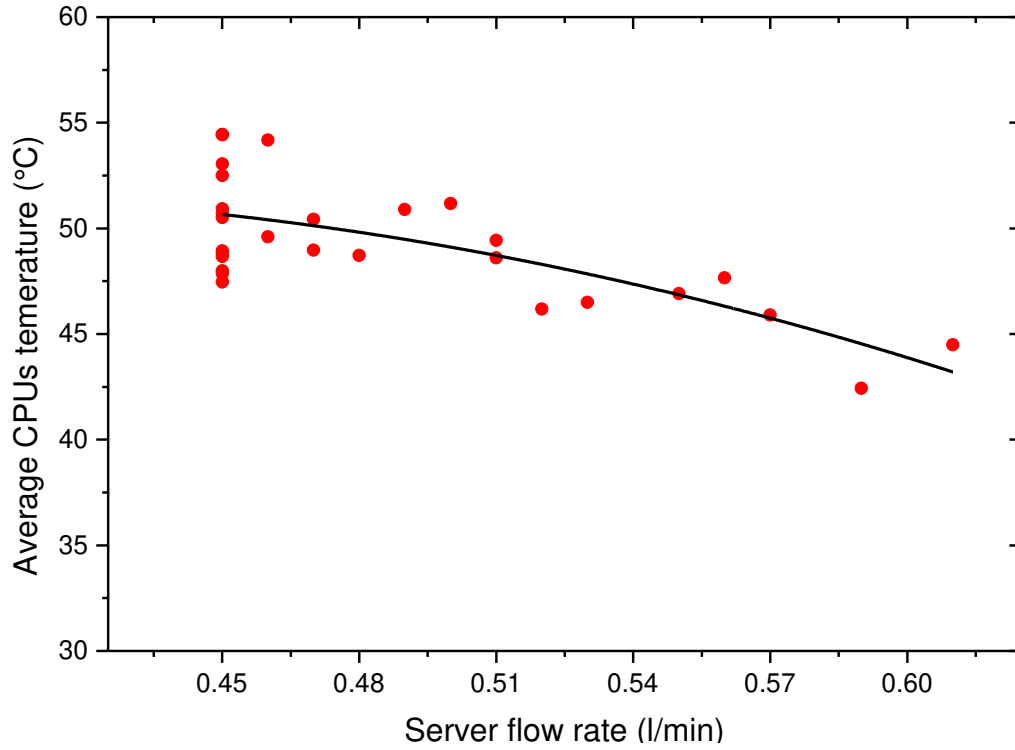


**Figure 15 Average CPUs temperature as a function of the server flow rate at 100% stress level of the rack.**

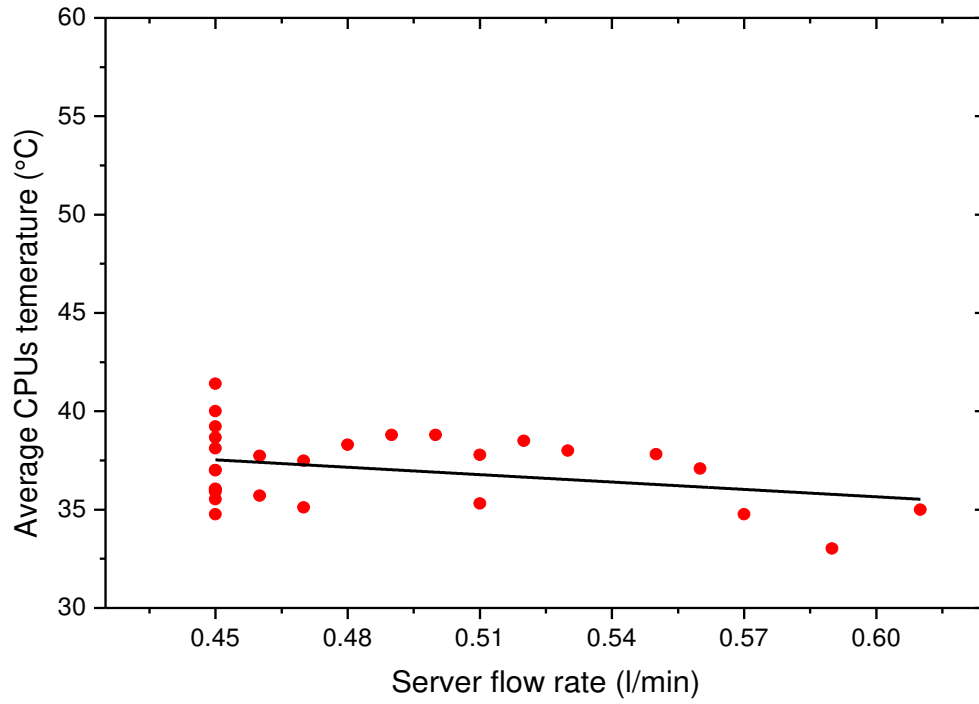


**Figure 16 Average CPUs temperature as a function of the server flow rate at idle operation of the rack.**

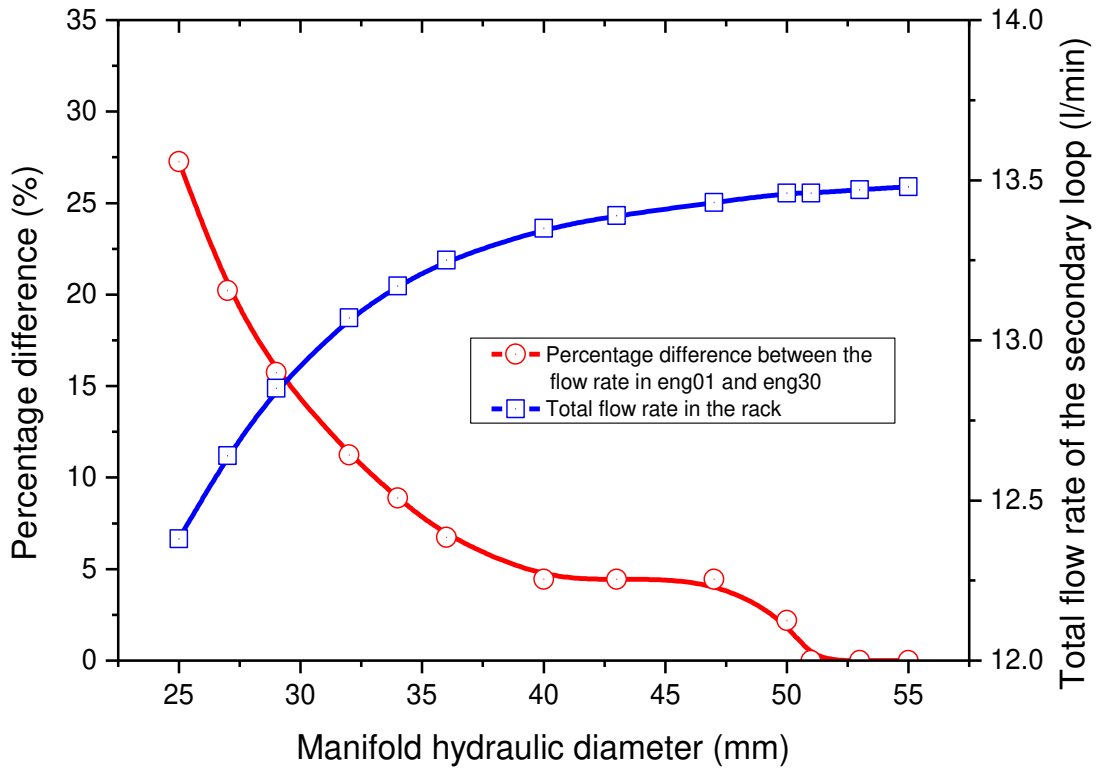


**Figure 17 Manifold size effect on the flow distribution in the central pumping configuration (the CHx pumps are running only).**

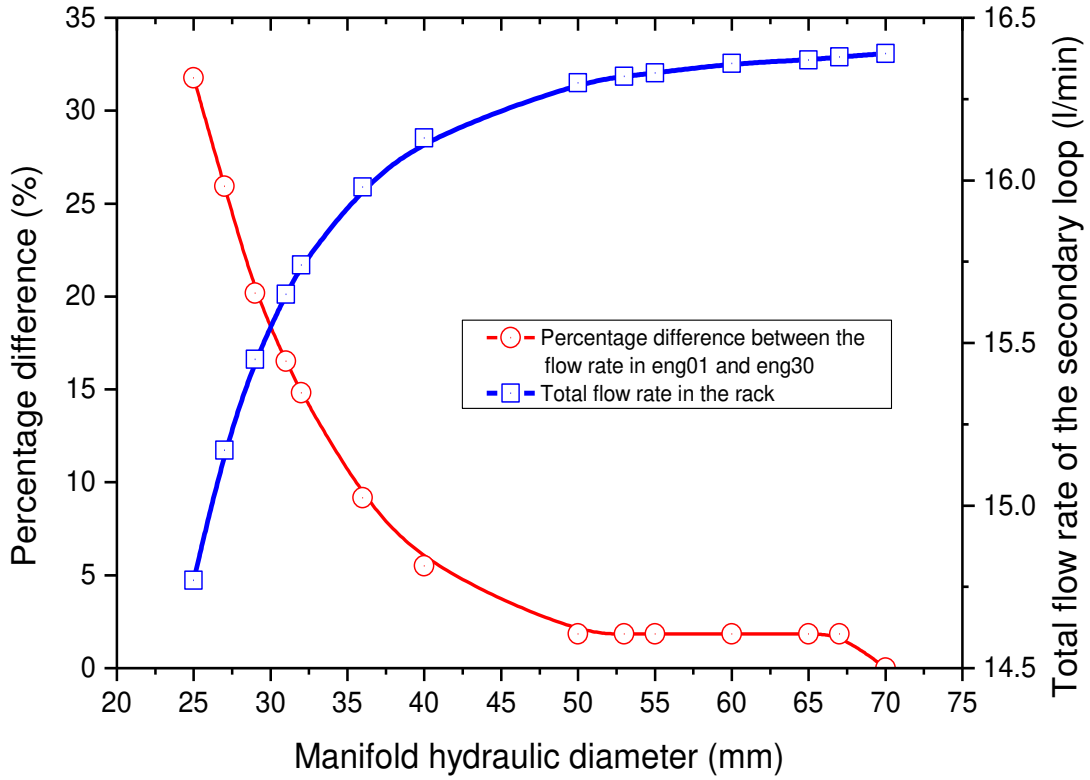


**Figure 18 Manifold size effect on the flow distribution in the distributed pumping configuration (the CHx pumps are kept running as well as the small pumps at the CPUs).**

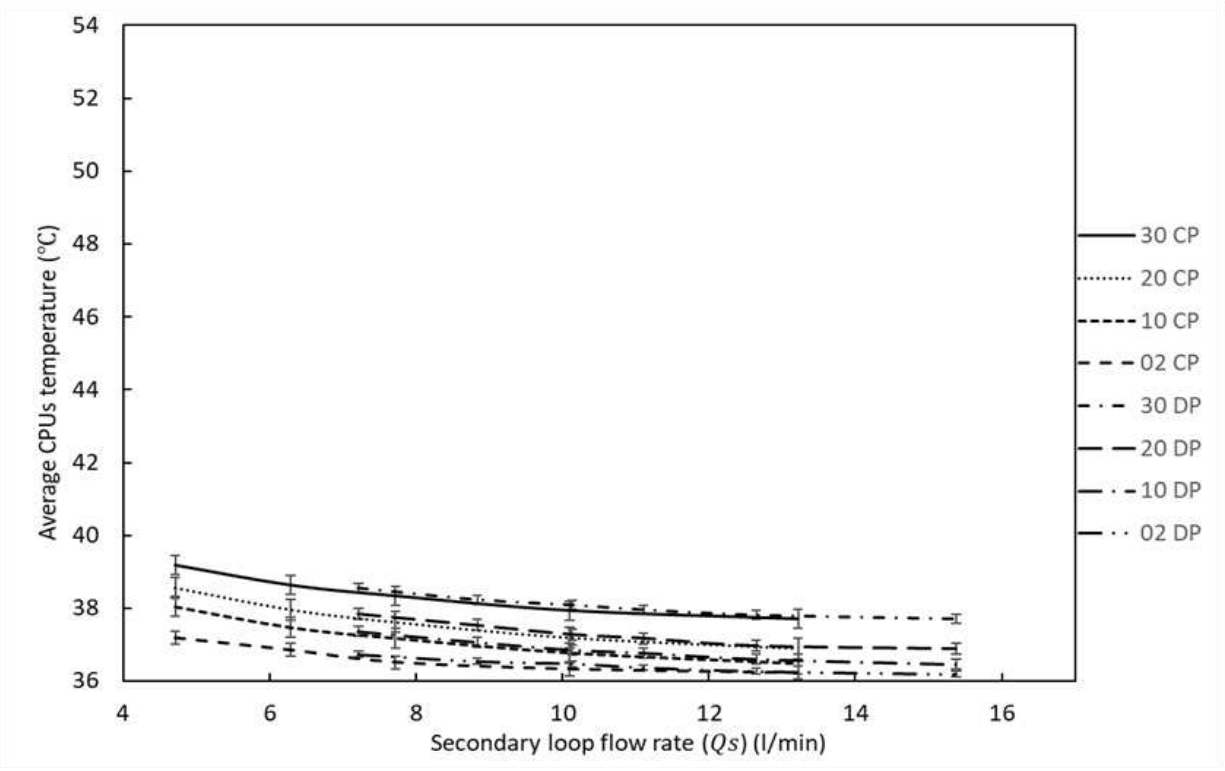


**Figure 19 Average temperature of selected CPUs as a function of the secondary loop flow rate for the idle operation of the rack. (The numbers in the legend are referred to the servers number from the top to the bottom of the rack while the CP and DP are referred to the centralised and distributed pumping configurations).**

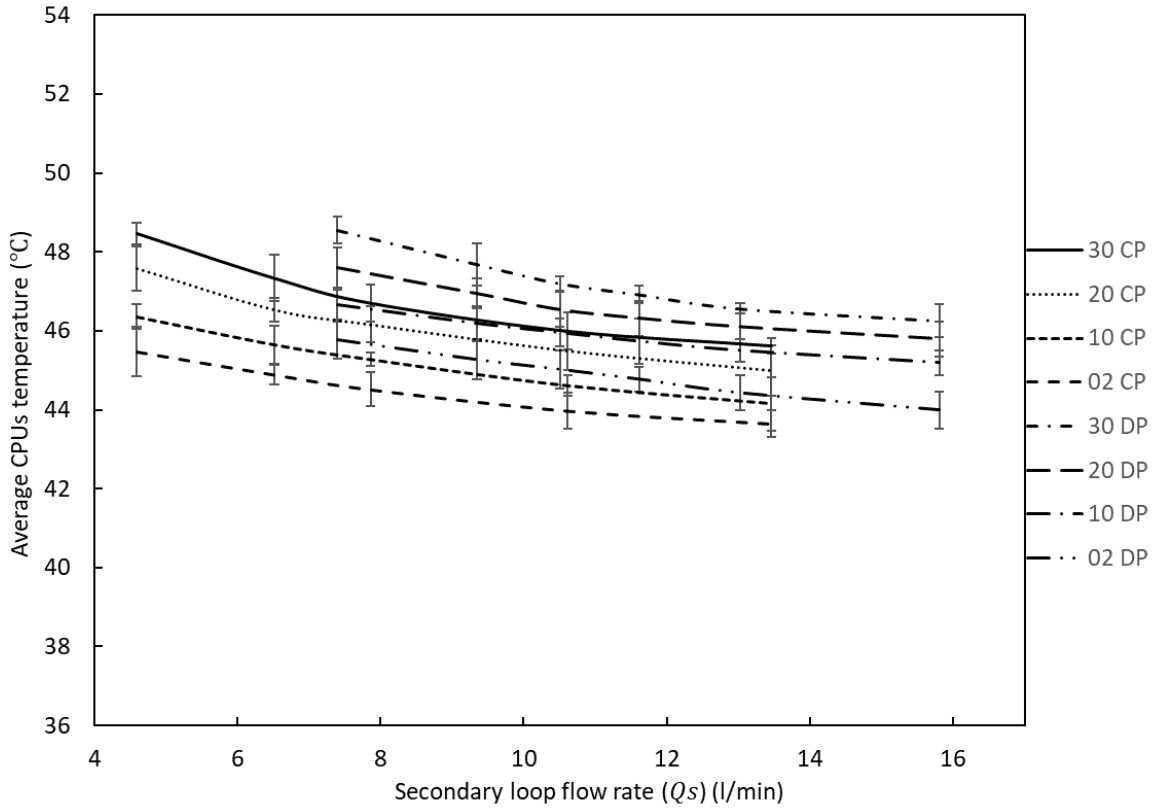


**Figure 18 Average temperature of selected CPUs as a function of the secondary loop flow rate for the 50% workload. (The numbers in the legend are referred to the servers number from the top to the bottom of the rack while the CP and DP are referred to the centralised and distributed pumping configurations).**

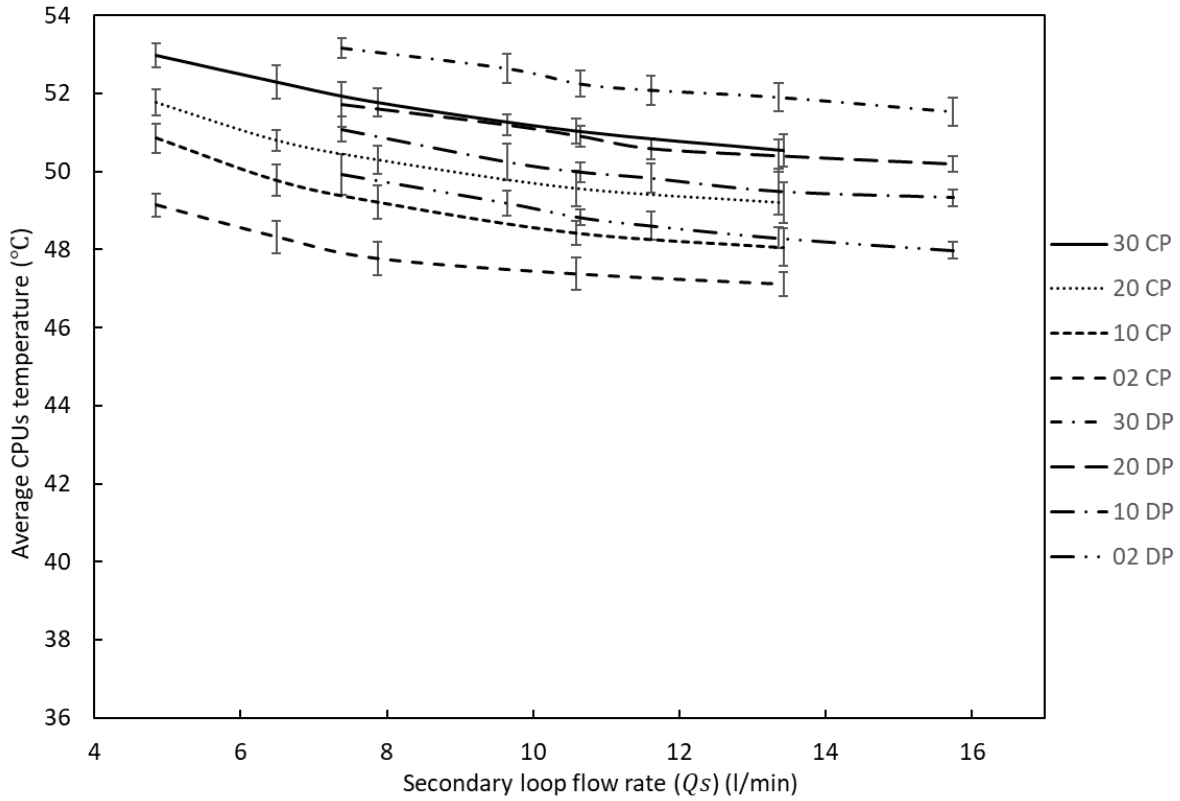


**Figure 209 Average temperature of selected CPUs as a function of the secondary loop flow rate for the 100% workload. (The numbers in the legend are referred to the servers number from the top to the bottom of the rack while the CP and DP are referred to the centralised and distributed pumping configurations).**

## BIOGRAPHICAL INFORMATION



**Dr. Mustafa Kadhim**, is Doctor of ThemoFluids specialising in data centre liquid cooling. He obtained his PhD in 2018 from the University of Leeds. His project was to engineer high-performance operation of the IT equipment. This is part of his general interest of becoming a world-leading expert in thermal management of data centres. Mustafa current career is in industry to engineer data centres towards lower power consumption, higher computational performance and energy reuse.



**Professor Nikil Kapur** is Professor of Applied Fluid Mechanics at the School of Mechanical Engineering, University of Leeds. His research interests span fundamental fluid mechanic phenomena covering multiphase systems through to industrially related studies. His work is highly disciplinary covering areas as diverse as cell growth, protein aggregation, the design of flow reactors, crystallisation and the design of flow equipment. He draws on computational and experimental techniques to further the understanding of fluid mechanic related challenges.



**Dr. Jon Summers** is currently on a study leave from the School of Mechanical Engineering at the University of Leeds in the role of Scientific Leader in Data Centres at Research Institutes of Sweden and an Adjunct Professor in Fluid Mechanics at Lulea University of Technology. Jon has focussed his attention towards holistic data centre research to bridge the gap between the facility and the Information

Technology, to enable innovative integrated approaches against the backdrop of increasing energy demand. During the last 25 years, Jon has worked on many government and industry funded research and development projects, many of which in the last 8 years have been directed towards energy efficient thermal management of data centres and microelectronics.



**Professor Harvey Thompson** (HT) FIMechE is Professor of Computational Fluid Dynamics (CFD) and Head of the School of Mechanical Engineering at the University of Leeds. He has published over 170 papers in the areas of CFD, Heat Transfer and Multi-disciplinary Design Optimisation (MDO) of engineering products and processes and has collaborated

with leading companies in the aerospace, automotive and food sectors. His recent research in CFD-enabled flow optimisation has been focussed in electronics and machine tool cooling systems and is finding application in a range of other biological, chemical and nuclear flow processing systems.